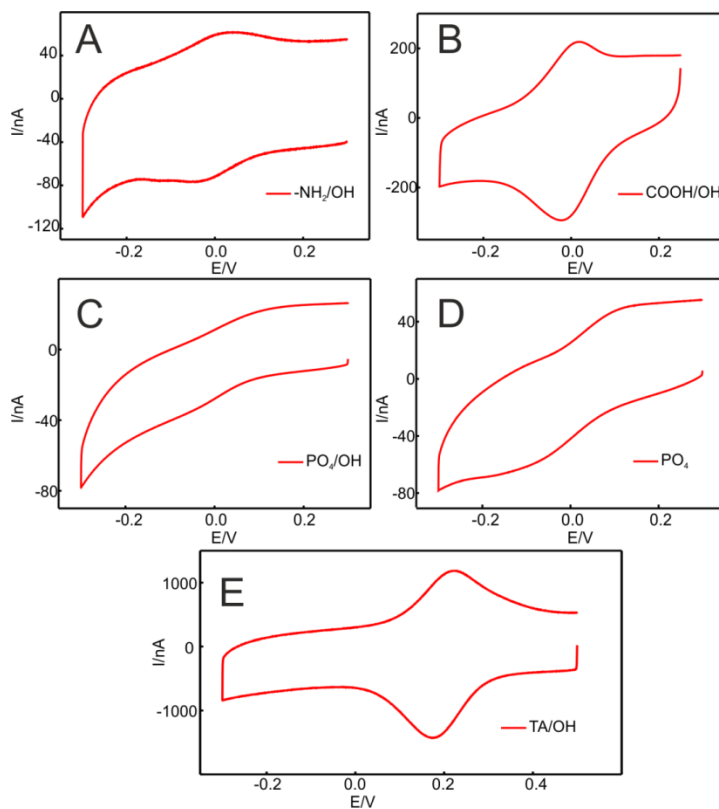


## Electronic Supplementary Information

### Specific Methionine Oxidation of Cytochrome *c* in Complexes with Zwitterionic Lipids by Hydrogen Peroxide: Potential Implications for Apoptosis

Daiana A. Capdevila, Waldemar A. Marmisolé, Florencia Tomasina, Verónica Demicheli, Magdalena Portela, Rafael Radi and Daniel H. Murgida



**Figure S1.** Cyclic voltammograms of Cyt-*c* adsorbed on Au electrodes coated with NH<sub>2</sub>/OH-SAM (A), COOH/OH-SAM (B), PO<sub>4</sub>/OH-SAM (C), PO<sub>4</sub>-SAM (D) and TA-SAM (E). All measurements were performed 10 mM phosphate buffer, pH 7, at room temperature and 0.05 V s<sup>-1</sup> scan rate.

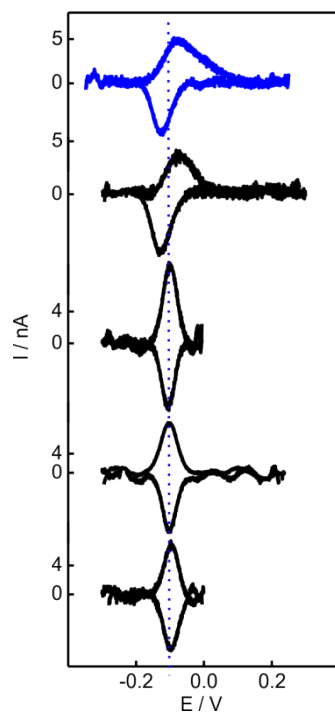


**Figure S2.** Background corrected voltammetric responses of SO-Cyt species generated in situ on NH<sub>2</sub>-SAMs determined in the presence of different complexing agents. From top to bottom: without complexing agent, 0.1 mM DTPA, 1 M sodium azide, 0.1 M imidazole, and 70 mM methionine. All measurements were performed 10 mM phosphate buffer, pH 7, at room temperature.

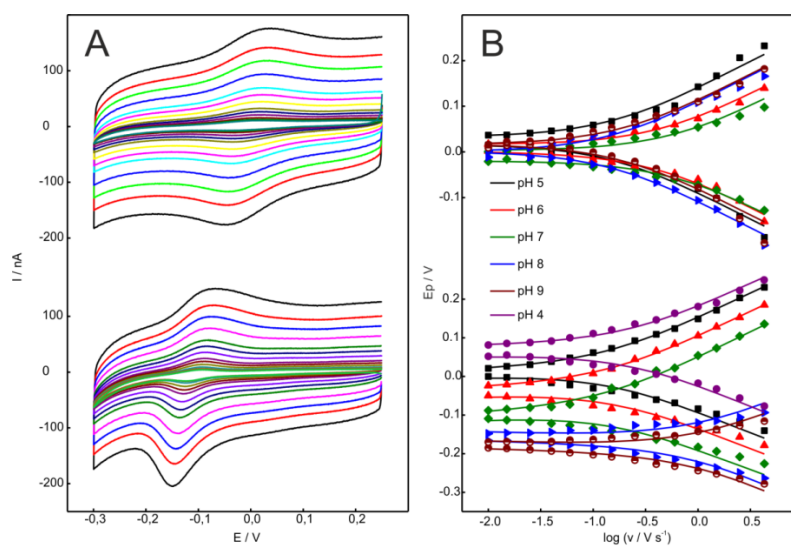


**Figure S3.** (A) CV of Cyt-c (top) and in situ generated SO-Cyt (bottom) adsorbed on a Au electrode coated with an NH<sub>2</sub>-SAM. Measurements were performed 10 mM phosphate buffer (pH 7) at variable scan rates (0.01-0.15 Vs<sup>-1</sup>). (B) Peak potentials as a function of the scan rates for Cyt-c (top) and in situ generated SO-Cyt on NH<sub>2</sub>-SAMs as a function of pH (see color code in the figure). The symbols are experimental values and the lines represent the best fits to Laviron's equation for quasi-reversible adsorbed electrochemical systems.

**Table S1.** ET parameters of Cyt-c and in situ generated SO-Cyt on NH<sub>2</sub>-SAMs.

pH	Cyt-c		SO-Cyt	
	$\ln(k_{app}/s^{-1})$	$E^{0'}/V$	$\ln(k_{app}/s^{-1})$	$E^{0'}/V$
4	-	-	3.5	0.079
5	2.4	0.026	2.1	0.030
6	6.3	0.004	2.3	-0.015
7	7.1	-0.013	2.2	-0.119
8	2.1	0.001	1.4	-0.170
9	3.0	0.016	1.5	-0.192

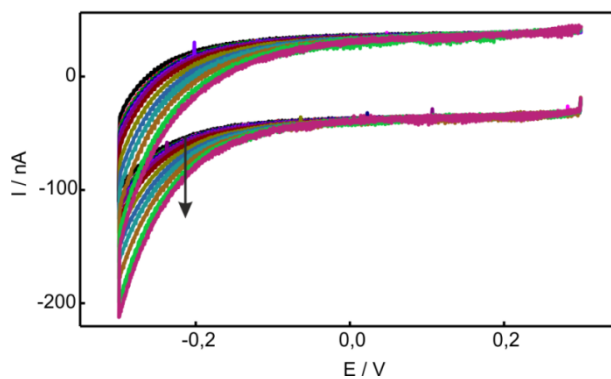


**Figure S4.** Cyclic voltammograms of Au electrodes coated with NH<sub>2</sub>-SAMs recorded in the absence of Cyt-c and in the presence of increasing amounts of H<sub>2</sub>O<sub>2</sub>, from 0 mM to 100 mM.

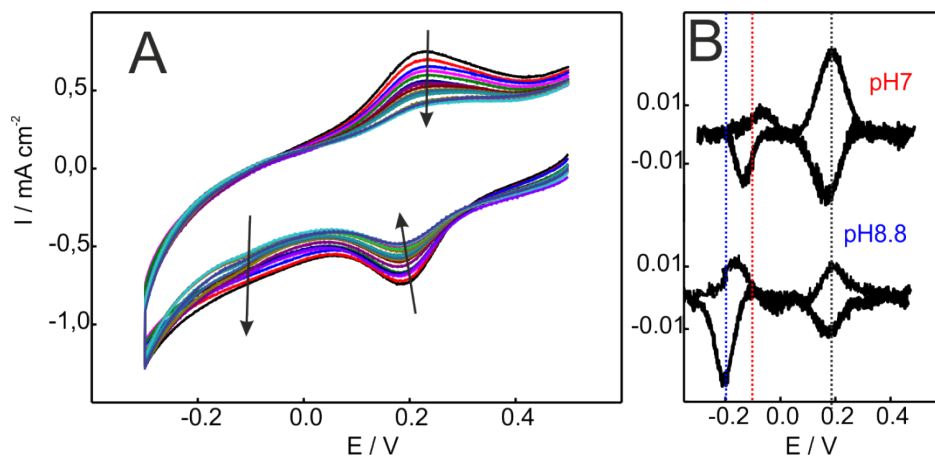


**Figure S5.** (A) Cyclic voltammograms of Cyt-c immobilized on a TA-SAM in the presence of increasing concentrations of H<sub>2</sub>O<sub>2</sub> from 0 to 2 mM as indicated by the arrows. All the experiments were performed in phosphate buffer, pH 7, at 0.05 Vs<sup>-1</sup>. (B) Background corrected voltammetric responses of Cyt-c at two different pH values obtained in the absence of H<sub>2</sub>O<sub>2</sub> after treatment with H<sub>2</sub>O<sub>2</sub> of the protein adsorbed on TA-SAMs. The dashed lines indicate the reduction potential of the SO-Cyt couple at the two pH values.

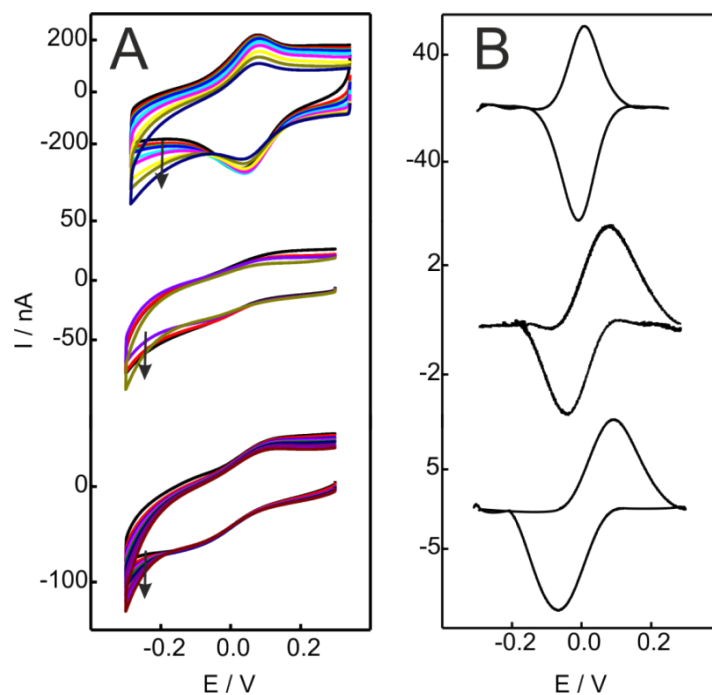


**Figure S6.** A. Cyclic voltammograms of Cyt-c adsorbed on Au electrodes coated with different SAMs. From top to bottom: COOH/OH-SAM, PO<sub>4</sub>/OH-SAM and PO<sub>4</sub>-SAM. The arrows indicate increasing H<sub>2</sub>O<sub>2</sub> concentrations from 0 up to 2 mM. All the experiments were performed in phosphate buffer, pH 7, at 0.05 Vs<sup>-1</sup>. B. Background corrected voltammetric response from Figure S6A.

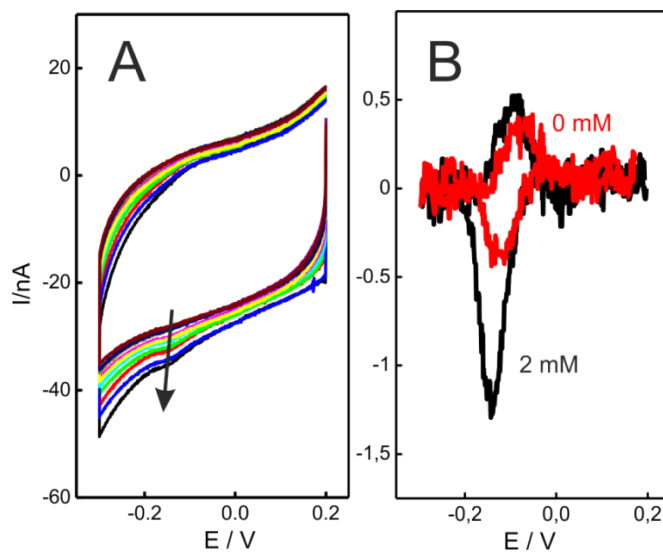


**Figure S7.** A. Voltammetric response of Cyt-c pre-treated with 1 mM H<sub>2</sub>O<sub>2</sub> in the presence of 5mM PE/PC and subsequently adsorbed on an Au electrode coated with NH<sub>2</sub>-SAM. The arrow indicates the rise of the cathodic currents in the presence of increasing concentrations of H<sub>2</sub>O<sub>2</sub> from 0 to 3 mM. All the experiments were performed in phosphate buffer, pH 7, at 0.05 Vs<sup>-1</sup>. B. Background corrected voltammetric response from Figure S7A. H<sub>2</sub>O<sub>2</sub> concentration: 0 (Red) to 3 mM (Black).

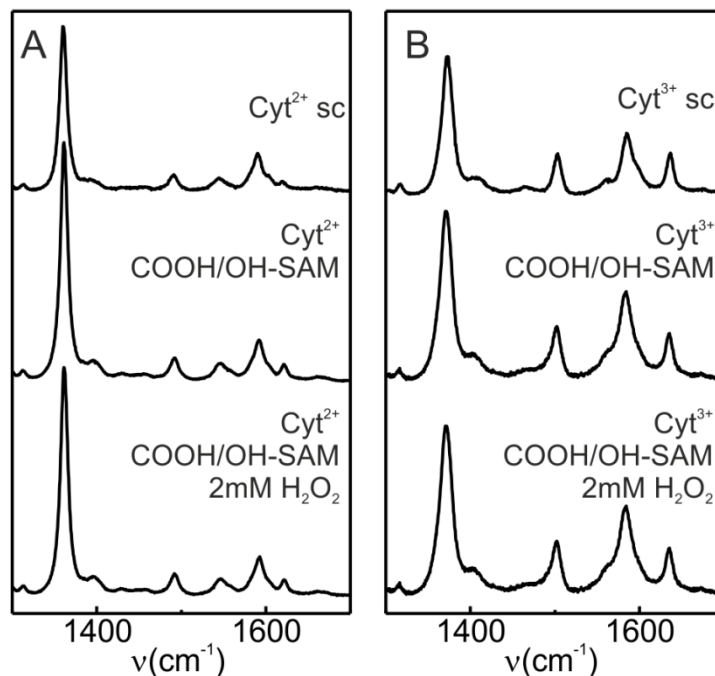


**Figure S8.** RR spectra of native Cyt-c in solution and SERR of Cyt-c adsorbed on Ag electrodes coated with COOH/OH-SAMs. SERR spectra were recorded before and after treatment with 2 mM H<sub>2</sub>O<sub>2</sub>. Panels (A) and (B) correspond to the ferrous and ferric forms, respectively. For RR experiments in solution sodium dithionite and potassium ferricyanide were employed as reducing and oxidizing agents. SERR measurements were performed under reducing (-0.3 V) and oxidizing (+0.15 V) applied potentials, respectively.

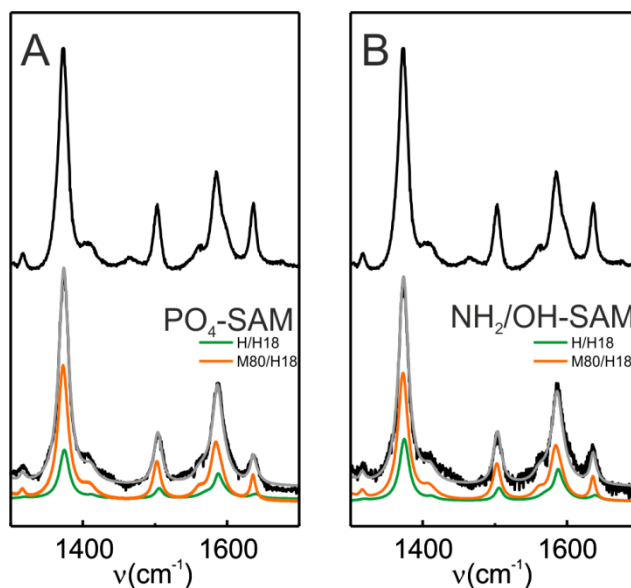


**Figure S9.** RR spectra of ferricyanide oxidized Cyt-c in solution (top) and SERR spectra of electrochemically oxidized Cyt-c adsorbed on Ag electrodes coated with two different SAMs: (A) PO<sub>4</sub>-SAM and (B) NH<sub>2</sub>/OH-SAM. Black lines: experimental spectra. Orange lines: six-coordinated low spin native spectral component (M80/H18). Green line: six-coordinated bis-His spectral component (H/H18). Gray line: overall spectral fit. All the experiments were performed in 20 mM phosphate buffer, pH 7.

**Table S2.** Resonance Raman spectral parameters of the different variants of ferric forms of cytochrome *c* employed for the component analysis of spectra recorded under 413 nm excitation. Relative intensities are shown in brackets. The spectral components for the Met/His and Lys/His species were obtained from Cyt-*c* spectra in 20 mM Hepes buffer solution at pH 7 and 10 respectively. His/His spectral components were obtained from mixtures of Cyt-*c* and cardiolipin in 20 mM Hepes pH 7 buffer solution, as reported in reference 8. OH-/His spectral components were obtained from a solution of M80A point mutant in 20 mM Hepes pH 7 buffer solution.

<i>Band</i>	<i>Axial coordination</i>			
	Met/His	His/His	Lys/His	OH-/His
v4	1371.8 cm <sup>-1</sup> (1.00)	1373.4 cm <sup>-1</sup> (1.00)	1374.8 cm <sup>-1</sup> (1.00)	1373.8 cm <sup>-1</sup> (1.00)
v3	1501.9 cm <sup>-1</sup> (0.28)	1505.8 cm <sup>-1</sup> (0.20)	1503.8 cm <sup>-1</sup> (0.33)	1503.1 cm <sup>-1</sup> (0.34)
v2	1583.9 cm <sup>-1</sup> (0.34)	1587.6 cm <sup>-1</sup> (0.37)	1586.7 cm <sup>-1</sup> (0.37)	1586.7 cm <sup>-1</sup> (0.41)
v10	1635.1 cm <sup>-1</sup> (0.18)	1639.6 cm <sup>-1</sup> (0.08)	1637.7 cm <sup>-1</sup> (0.20)	1635.1 cm <sup>-1</sup> (0.06)

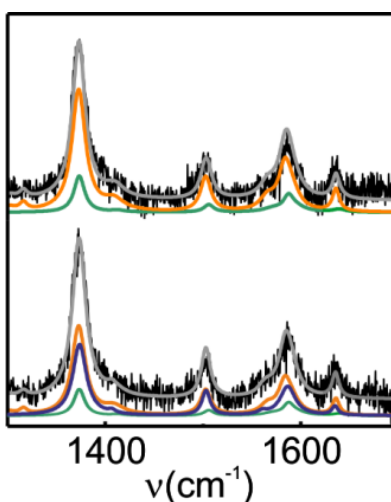


**Figure S10.** SERR spectra of Cyt-*c* adsorbed on a Ag electrode coated with NH<sub>2</sub>/OH-SAM recorded before (top) and after (bottom) treatment with 1 mM H<sub>2</sub>O<sub>2</sub>. Spectra were recorded at 0.15 V in phosphate buffer, pH 7. H<sub>2</sub>O<sub>2</sub> was added while cycling from -0.3 V to 0.1 V at 0.05 Vs<sup>-1</sup>.

**Synthesis and characterization of SO-Cyt.** Selective sulfur oxidation of Met80 was performed using chloramine-T as oxidizing reagent.<sup>1,2</sup> Briefly, equal volumes of horse heart Cyt-*c* (1 mM) and chloramine-T (5 mM) were mixed in 10 mM Tris-HCl (pH 8.4). After 3 hours at room temperature, the mixture was thoroughly washed with 10 mL of 10 mM phosphate buffer, pH 7, using Amicon 10 kDa centrifugal filters. The progress of the reaction was monitored by UV-vis, looking at the continuous decrease of the 695 nm band, which is indicative of the Met-Fe bond (Fig. S11).

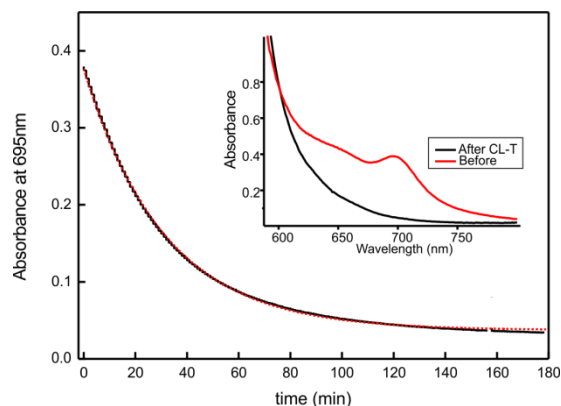


**Figure S11.** Decay of the 695 nm band of Cyt-c after treatment with chloramine-T. Inset: spectrum in the region of the 695-nm band before and after the reaction.

The reaction mixture was separated using a cation exchange sulfopropyl-TSK preparative column (21.5 mm inner diameter; 15.0 cm length; Tosoh Biosep) in order to obtain purified SO-Cyt species. Different chromatographic peaks were obtained (A, B and C) as shown in Fig. S12. Peak A and Cyt-c have identical elution times. Fractions B and C, on the other hand, are characterized by UV-vis spectra that lack the characteristic 695 nm band and, in addition, present blue shifted Soret bands (Fig. S12B).

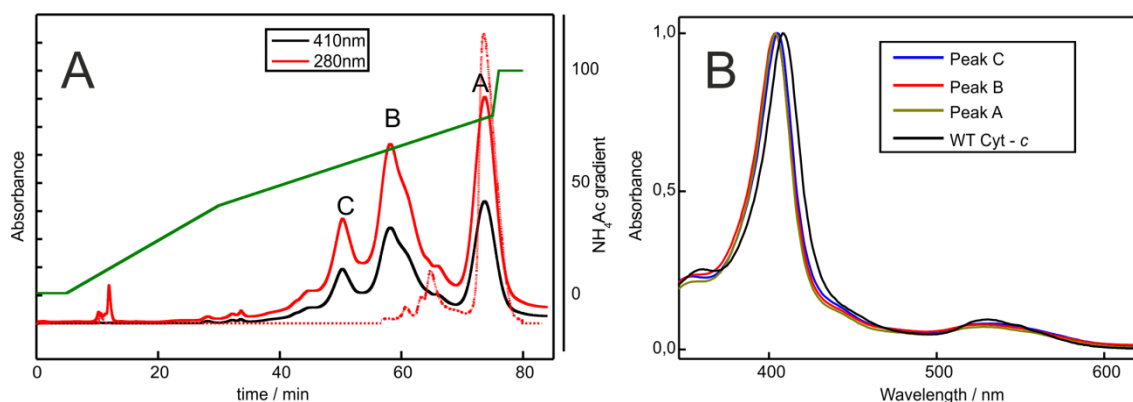


**Figure S12.** (A) Cation-exchange HPLC analysis of Cyt c after treatment with chloramine T. Cyt-c (3 mM) in 100 mM Tris-HCl buffer (pH 8.4) was treated with chloramine T (2.5 mM). The reaction mixture (9,2 mg of protein) was passed through the HPLC preparative column and the peaks (A, B and C) were collected manually. For comparison the chromatogram of native Cyt-c is shown as a red dashed line. (B) UV-Vis Spectra of the different fractions.

Peroxidase activity of the different fraction was assessed with Amplex UltraRed Reagent. All fractions showed increased activity compared to native Cyt-c (Table S3). Peak B showed the highest activity, consistent with the SO-Cyt species.

**Table S3.** Peroxidase activity of the different fractions. The fluorescence of the oxidation product of Amplex UltraRed Reagent, resorufin, was monitored at  $\lambda_{em} = 585$  nm with  $\lambda_{ex} = 570$  nm during 60 min. 0.5  $\mu$ M Cyt-c was incubated in HEPES (10 mM plus 100  $\mu$ M DTPA), pH 7. Then, 50  $\mu$ M Amplex Red and 25  $\mu$ M H<sub>2</sub>O<sub>2</sub> were added in HEPES (100 mM plus 100  $\mu$ M DTPA) pH 7. The reaction rate was determined by linear fit of the fluorescence intensity. Activities are expressed as percentage of the control (native Cyt-c).

Fraction	Activity % of control
Native Cyt-c	100
A	300
B	1300
C	500

The different fractions were characterized by RR spectroscopy under Soret band excitation (Fig S13). Fraction C presents has a large contribution of high spin species consistent with the presence of denatured protein.

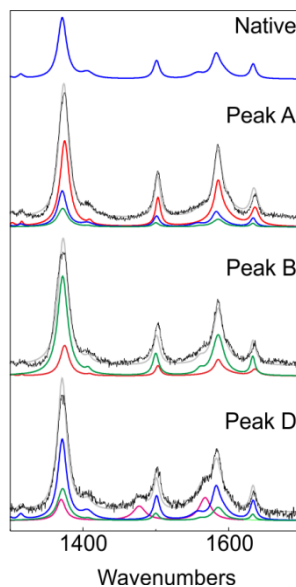


**Figure S13.** RR spectra of the different fractions obtained by HPLC after treatment of Cyt-c with chloramine-T. Blue: Met/His component. Red: Lys/His component. Green: OH/His component. Magenta: H<sub>2</sub>O/His component.

Fraction B shows a large proportion of OH/His spectral component as well as the highest peroxidase activity and, therefore, is the most likely candidate for SO-Cyt.

The purified SO-Cyt (Peak B) was analyzed by MALDI-TOF MS in order to verify the site of oxidation and to rule out other modifications (Fig S14). For that purpose the sample was



digested with trypsin (sequence grade, Promega) in 50 mM argon-saturated  $\text{NH}_4\text{HCO}_3$  buffer, as described elsewhere.<sup>1</sup>

Met80 oxidation was confirmed by the appearance of the +16 Da peak in the peptide MIFAGIK, which corresponds to the addition of an oxygen atom (Table S4).<sup>1</sup> Met65 oxidation was also confirmed by the presence of the +16 Da peak in the peptide EETLMEYLENPK (Table S3). Both modifications were observed for all the fractions.

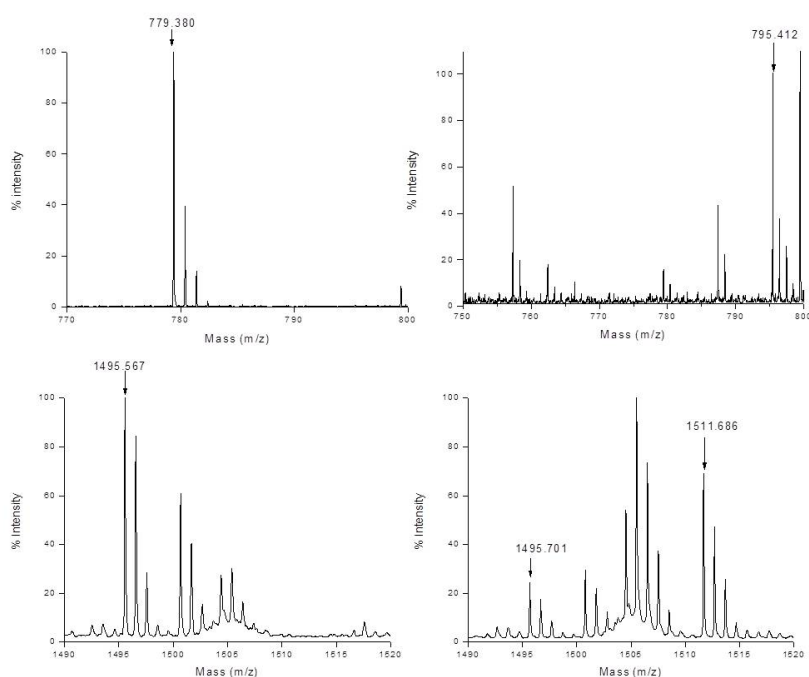


**Figure S14.** MALDI-TOF mass spectra of tryptic digests of Cyt-c. Left: native Cyt-c. Right: fraction B. The protein solution was diluted to a concentration of 25  $\mu\text{M}$  with 50 mM ammonium bicarbonate buffer (pH 7.9 and argon-saturated). Cleavage was carried out with trypsin in a 1:50 ratio (w/w) at 37 °C for 12 hrs under argon saturation. Prior to MS analyses, samples were desalted using C18 reverse phase micro-columns (Omixon®Tips, Varian) and eluted directly onto the sample plate for MALDI-MS with CHCA matrix solution in aqueous 60% ACN containing 0.1% TFA.

**Table S4.** Monoisotopic molecular masses of the chromatographic fraction B of Cyt-c treated with chloramine-T.

	Peptide sequence	Theoretical mass (Da) [(M+H) <sup>+</sup> ]	Detected mass (Da) [(M+H) <sup>+</sup> ]	$\Delta\text{M}$ (Da)	Modified residue
Fraction B	MIFAGIK	779.378	795.472	16.094	Met80
	EETLMEYLENPK	1495.571	1511.764	16.193	Met65

**Redox behavior of the M80A mutant of Cyt-c.** The M80A variant was obtained according to the procedure described elsewhere.<sup>3</sup> For CV measurements the protein was covalently attached to a Au electrode coated with a COOH-SAM by using CMC (20 mg/10 mL) and NHS (6 mg/10 mL) as described previously.<sup>4</sup> The results are shown in Figure S 14.

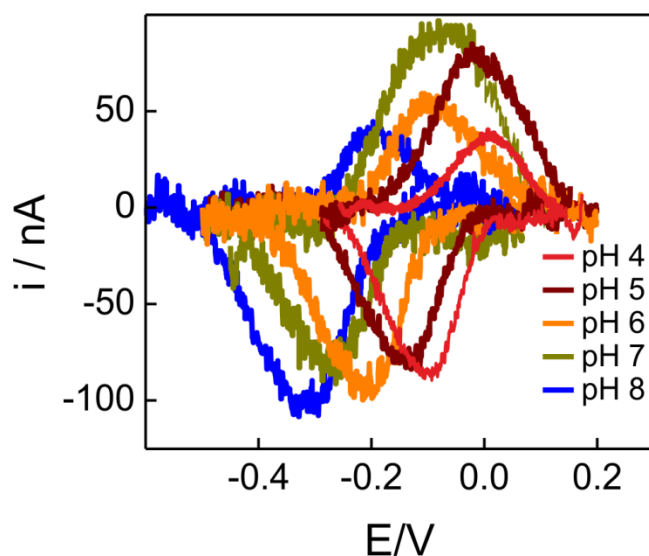
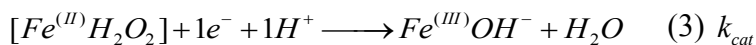
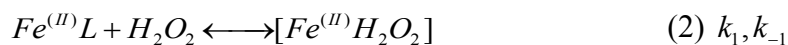
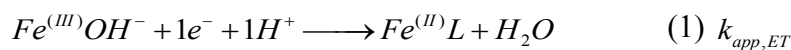
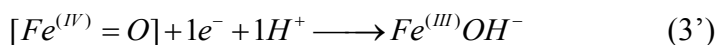
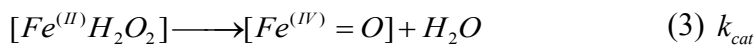


**Figure S15.** Cyclic voltammograms of the M80A mutant covalently attached to a COOH-SAM recorded at different pH values.

**Derivation of electrocatalytic parameters.** The experimental results are consistent with the following minimal reaction scheme:



The third reaction, in turn, can be described as a two steps process involving a ferryl intermediate:<sup>5 6</sup>



As the redox potential of the ferryl species is very positive<sup>7</sup> the reduction step (3') is expected to be fast and, therefore, step (3) is likely to be rate limiting.

The current generating steps are (1) and (3), so current density can be calculated as

$$j = F(v_1 + v_3)$$

$$v_1 = k_{app,ET}[Fe^{(III)}OH^-]$$

$$v_3 = k_{cat}[Fe^{(II)}H_2O_2]$$

where  $v$  is the rate of each step ( $\text{mol s}^{-1} \text{cm}^{-2}$ ).

Assuming steady-state conditions for the intermediate  $[Fe^{(II)}H_2O_2]$  and considering that the surface concentration of Cyt-c species,  $[Fe]$ , remains constant:

$$[Fe]_0 = [Fe^{(II)}H_2O_2]_{SS} + [Fe^{(II)}H_2O] + [Fe^{(III)}OH^-]$$

$$\text{the rate of step (3) becomes: } v_3 = \left(1 - \frac{[Fe^{(III)}OH^-]}{[Fe]_0}\right) [Fe]_0 \left(\frac{k_{cat}[H_2O_2]}{K_M + [H_2O_2]}\right)$$

$$\text{where } K_M = (k_{-1} + k_{cat}) / k_1$$

$$\text{Then, } j = F[Fe]_0 \left( k_{app,ET} \frac{[Fe^{(III)}OH^-]}{[Fe]_0} + \left(1 - \frac{[Fe^{(III)}OH^-]}{[Fe]_0}\right) \left(\frac{k_{cat}[H_2O_2]}{K_M + [H_2O_2]}\right) \right)$$

In the absence of substrate, for a reversible or quasi-reversible redox couple, the peak

$$\text{current corresponds to } \frac{[Fe^{(III)}OH^-]}{[Fe]_0} = 0.5 \text{ and } j_{p,0} = 0.5Fk_{app,ET}[Fe]_0$$

By assuming that this condition is also valid in the presence of the substrate, then:

$$j_p = 0.5F[Fe]_0 \left( k_{app,ET} + \left(\frac{k_{cat}[H_2O_2]}{K_M + [H_2O_2]}\right) \right) \text{ and } j_p - j_{p,0} = 0.5F[Fe]_0 \left(\frac{k_{cat}[H_2O_2]}{K_M + [H_2O_2]}\right)$$

The protein concentration can be evaluated from the integrated charge in the absence of catalysis  $Q_0 = F[Fe]_0$

$$\text{Then we obtain a Michaelis-Menten-like equation: } j_p - j_{p,0} = 0.5Q_0 \left(\frac{k_{cat}[H_2O_2]}{K_M + [H_2O_2]}\right)$$

By fitting the experimental cathodic currents obtained as a function of H<sub>2</sub>O<sub>2</sub> concentration we obtain  $K_M = 0.44 \pm 0.07$  mM and  $k_{cat} = 1.8 \pm 0.6$  s<sup>-1</sup> for *in-situ* generated SO-Cyt (Fig. 5), where  $k_{cat}$  was obtained from the limiting current density.

## References

1. Y.-R. Chen, L. J. Deterding, B. E. Sturgeon, K. B. Tomer, and R. P. Mason, *J. Biol. Chem.*, 2002, **277**, 29781–91.
2. J. Pande, K. Kinnally, K. K. Thallum, B. Verma, Y. Myer, L. Rechsteiner, and H. Bosshard, *J. Protein Chem.*, 1987, **6**.
3. L. C. Godoy, C. Muñoz-Pinedo, L. Castro, S. Cardaci, C. M. Schonhoff, M. King, V. Tórtora, M. Marín, Q. Miao, J. F. Jiang, A. Kapralov, R. Jemmerson, G. G. Silkstone, J. N. Patel, J. E. Evans, M. T. Wilson, D. R. Green, V. E. Kagan, R. Radi, and J. B. Mannick, *Proc. Natl. Acad. Sci. U. S. A.*, 2009, **106**, 2653–8.
4. H. K. Ly, M. A. Marti, D. F. Martin, D. Alvarez-Paggi, W. Meister, A. Kranich, I. M. Weidinger, P. Hildebrandt, and D. H. Murgida, *Chemphyschem*, 2010, **11**, 1225–35.
5. H. B. Dunford, *Coord. Chem. Rev.*, 2002, **234**, 311–318.
6. S. Águila, A. M. Vidal-Limón, J. B. Alderete, M. Sosa-Torres, and R. Vázquez-Duhalt, *J. Mol. Catal. B Enzym.*, 2013, **85-86**, 187–192.
7. G. Battistuzzi, M. Bellei, C. A. Bortolotti, and M. Sola, *Arch Biochem Biophys*, 2010, **500**, 21–36.
8. J. M. Bradley, G. Silkstone, M. T. Wilson, M. R. Cheesman and J. N. Butt, *J. Am. Chem. Soc.*, 2011, **133**, 19676.